Acta Geochim (2023) 42(2):183–194
https://doi.org/10.1007/s11631-023-00594-x

ORIGINAL ARTICLE

The breakdown of diopside to (Ca, Mg)SiO_3 perovskite–(Mg, Ca, Fe)SiO_3 glass–(Mg, Ca)SiO_3 glass–(Mg, Ca)SiO_3 majorite in a melt vein the Suizhou L6 chondrite

Xiande Xie[1] · **Xiangping Gu**[2]

Received: 15 December 2022 / Revised: 9 January 2023 / Accepted: 11 January 2023 / Published online: 2 February 2023

Abstract The Suizhou meteorite is a heavily shocked and melted vein-containing L6 chondrite. It contains a minor amount of diopside with a $(Ca_{0.419}Mg_{0.466}Fe_{0.088})SiO_3$ composition, and a shock-metamorphosed diopside grain associated with ringwoodite and lingunite was found in a melt vein of this meteorite. Our electron microprobe, transmission electron microscopic and Raman spectroscopic analyses revealed four silicate phases with different compositions and structures inside this shock-metamorphosed diopside grain, termed phase A, B, C and D in this paper. Phase A is identified as orthorhombic $(Ca_{0.663}Mg_{0.314})SiO_3$-perovskite which is closely associated with phase B, the vitrified $(Mg_{0.642}Ca_{0.290}Fe_{0.098})SiO_3$ perovskite. Phase D is assigned to be $(Mg_{0.578}Ca_{0.414})SiO_3$ majorite which is associated with phase C, the vetrified Ca-rich Mg-perovskite with a $(Mg_{0.853}Ca_{0.167})SiO_3$ composition. Based on high-pressure and high-temperature experiments, the diopside grain in the melt vein of the Suizhou meteorite would have experienced a *P–T* regime of 20–24 GPa and 1800 – > 2000 °C. Such *P–T* conditions are high enough for the decomposition of the diopside and the formation of four different silicate phases. The orthorhombic $(Ca_{0.663}Mg_{0.314})SiO_3$ perovskite found in the Suizhou L6 chondrite might be considered as the third lower-mantle silicate mineral after bridgmanite and davemaoite after the detailed analyses of its crystal structure and physical properties being completed.

Keywords Suizhou chondrite · Diopside · Shock metamorphism · (Ca, Mg)SiO_3-perovskite · (Mg, Ca, Fe)SiO_3 glass · (Mg, Ca)SiO_3 glass · (Mg, Ca)SiO_3 majorite

1 Introduction

Diopside is a monoclinic pyroxene mineral of $CaMgSi_2O_6$ composition. It is an important constituent silicate mineral in both pyrolite and basalt, and is believed to be one of the most abundant Ca-bearing minerals in the upper mantle. Numerous experimental studies on the phase relations of diopside $CaMgSi_2O_6$ under high pressures and high temperatures have been performed (Mao et al. 1977; Liu 1987; Tamai and Yagi 1989; Kim et al. 1994; Oguri et al. 1997; Irifune et al. 2000). The final results of all these experiments using diopside crystal as starting material under pressure up to 50 GPa are very similar, namely, the diopside $CaMgSi_2O_6$ had broken down into cubic $CaSiO_3$–perovskite and orthorhombic $MgSiO_3$–perovskite.

Although diopside is found widely in ordinary chondrites (Brearley and Jones 1998), its abundance is comparatively low, and very few occurrences of its high-pressure polymorph have been reported, namely, Ca-rich majorite as its high-pressure polymorph was found in just three ordinary chondrites: Yamato 75,100 (H6) (Tomioka and Kimura 2003), Tenham (L6) (Xie and Sharp 2007) and Villalbeto de la Pena (L6) (Martinez et al. 2019). No high-pressure polymorphs of diopside other than Ca-rich majorite were found in shocked meteorites up to now. In

✉ Xiande Xie
xdxie@gzb.ac.cn

[1] Key Laboratory of Mineralogy and Metallogeny / Guangdong Provincial Key Laboratory of Mineral Physics and Materials, Guangzhou Institute of Geochemistry, Chinese Academy of Sciences, Guangzhou 510640, China

[2] School of Geosciences and Info-Physics, Central South University, Changsha 410083, China

this paper, we report the finding of Ca-rich orthorhombic perovskite, vitrified (Mg, Ca, Fe)SiO_3 and (Mg, Ca)SiO_3 perovskites, and (Mg, Ca)SiO_3-majorite as the shock-induced decomposition products of diopside in a shock melt vein of the Suizhou L6 chondrite.

2 Samples and analytical methods

The Suizhou L6 chondrite fell on April 15, 1986, at Dayanpo, Suizhou City, Hubei Province, China. This meteorite consists of olivine, low-Ca pyroxene, diopside, plagioclase, FeNi-metal, troilite, merrillite, chlorapatite, chromite, ilmenite, pyrophanite, native copper, and shenzhuangite (Xie et al. 2001a, 2011, 2022; Xie and Chen 2016; Bindi and Xie 2017). The Suizhou meteorite was classified as a strongly shock-metamorphosed (S5) meteorite due to the presence of transformation of plagioclase to maskelynite (Xie et al. 2001a; 2011). This meteorite contains a few very thin shock-produced melt veins, and up to 17 high-pressure phases were identified inside or adjacent to melt veins. They are ringwoodite, majorite, lingunite, magnesiowüstite, majorite-pyrope$_{ss}$, akimotoite, ahrensite, TiO_2-II, and new high-pressure minerals tuite, xieite, chenmingite, wangdaodeite, hemleyite, asimowite, poirierite, hiroseite and elgoresyite (Xie et al. 2001a, b, 2002, 2003, 2011, 2016, 2019, 2022; Chen and Xie 2015, Chen et al. 2003, 2008; Ma et al. 2019; Xie and Chen 2016; Bindi et al. 2017, 2019, 2020, 2021; Tomioka et al. 2021).

Polished thin sections were prepared from fragments of the Suizhou meteorite. All observations and physical and chemical analyses are performed *in-situ* on thin sections. The mineral assemblages in polished thin sections of the samples were investigated by optical microscopy using a Leica DM 2500p microscope. A Shimadzu 1720 electron microprobe (EPMA) was used to study the mineral occurrence in back-scattered electron (BSE) mode, and to quantitatively determine the chemical composition of minerals using the wavelength dispersive technique at 15 kV accelerating voltage and beam current of 10 nA. Natural and synthetic phases of well-known compositions were used as standards**,** such as MgO for Mg, Fe_2O_3 for Fe, TiO_2 for Ti, Al_2O_3 for Al, $MnSiO_3$ for Mn, Cr_2O_3 for Cr, and the data were corrected using a ZAF program. Raman spectra of minerals in the polished thin sections were recorded with a Horiba Labram Aramis instrument. A microscope was used to focus the excitation beam (Ar + laser, 633 nm line) to 1 μm wide spots and to collect the Raman signal. Accumulations of the signal lasted 300 s. The laser power was 2 mW. Transmission electron microscopy (TEM) and selected area electron diffraction (SAED) were performed using FEI Titan G2 60-300 TEM operated at 300 kV accelerating voltage. The identifications of nano-sized phases were performed with an FEI Talos F200s scanning/transmission electron microscope (STEM) operating at 200 kV, equipped with a field emission gun. Bright-field, high-resolution bright-field, and STEM images of minerals as well as selected area electron diffractions in TEM were obtained from the samples. Compositional analysis of nano-sized crystallites and glass was conducted by using energy dispersive X-ray spectroscopy (EDXS) with an accelerating voltage of 200 kV, a beam current of 1 nA, and a beam size of ~ 5 nm in STEM mode. Accumulation time of X-ray signals was 5 s per analysis.

3 Results

3.1 Description of diopside in the Suizhou chondritic rock

Diopside is a rare silicate phase in the Suizhou meteorite. We only observed five diopside grains with $(Ca_{0.419}Mg_{0.466}Fe_{0.088}Ti_{0.007}Cr_{0.018}Na_{0.024})_{1.022}(Si_{0.977}Al_{0.014})_{0.991}O_3$ average composition in the Suizhou chondritic rock (Table 1). They have an irregular shape and dark-grey color (Fig. 1), and their Raman spectra show four strong peaks at 322–324, 390–391, 664–666, and 1012–1014 cm^{-1}, and some weaker bands at 134–135, 509–511 and 1044–1045 cm^{-1} (Fig. 2), which are identical to that of other natural diopsides (Kubicki et al. 1992).

Interestingly, an unusual diopside grain coexisting with lingunite and ringwoodite was found in a shock melt vein of the Suizhou meteorite (Fig. 3). Our EDXS analysis shows this grain is a CaMgFe-silicate (Fig. 4). The Raman spectrum of this grain shows a few very wide peaks which do not belong to diopside, but the three weak Raman peaks

Table 1 Chemical composition of diopside in the Suizhou chondritic rock (wt%)

No	1	2	3	4	5	Average
SiO_2	54.17	53.75	53.40	51.60	53.24	53.23
TiO_2	–	0.63	0.85	0.73	0.55	0.52
FeO	4.59	5.66	5.55	6.88	5.87	5.71
MgO	16.25	17.28	17.21	17.10	17.38	17.04
CaO	22.96	20.77	21.11	20.78	21.06	21.34
MnO	–	–	–	–	–	–
Al_2O_3	0.47	0.49	0.74	0.85	0.60	0.63
Cr_2O_3	0.85	1.23	1.33	1.52	1.20	1.23
Na_2O	0.58	0.69	0.66	0.90	0.59	0.68
Total	99.87	100.50	100.85	100.36	100.49	100.38

Formula: $(Ca_{0.419}Mg_{0.466}Fe_{0.088}Ti_{0.007}Cr_{0.018}Na_{0.024})_{1.022}(Si_{0.977}Al_{0.014})_{0.991}O_3$

Simplified formula: $(Ca_{0.419}Mg_{0.466}Fe_{0.088})\ Si_1O_3$

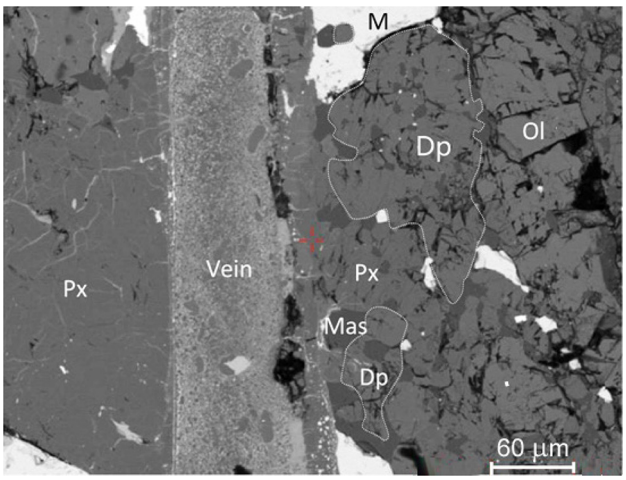

Fig. 1 Back-scattered electron image showing the occurrence of diopside (Dp) in the Suizhou meteorite. Vein = shock melt vein, Ol = olivine, Px = orthopyroxene, Mas = maskelynite, M = FeNi metal

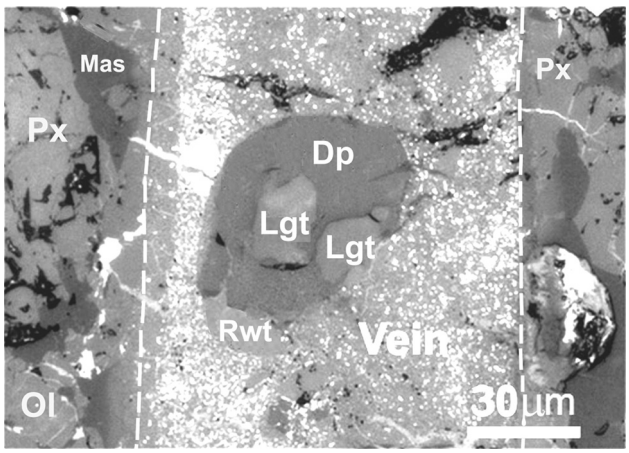

Fig. 3 Photomicrograph of the shock-metamorphosed diopside (Dp) grain in a shock melt vein (vein) of the Suizhou meteorite. Lgt = lingunite, Rwd = ringwoodite, Ol = olivine, Px = pyroxene, Mas = maskelynite

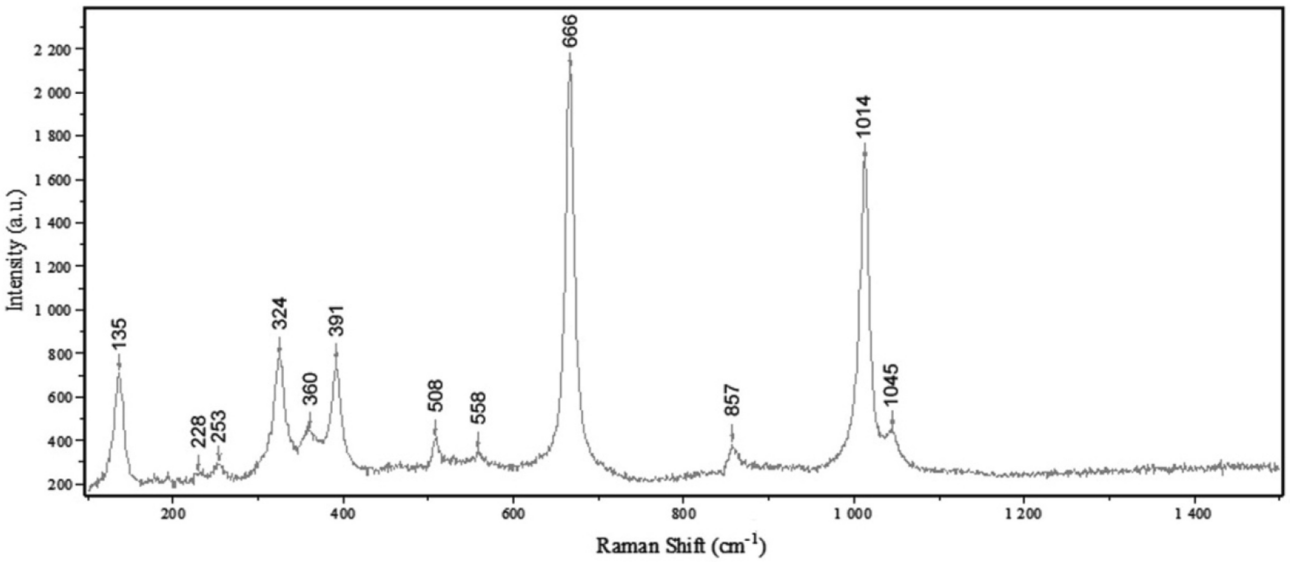

Fig. 2 Raman spectrum of a diopside grain in the Suizhou chondritic rock

at 1016,660 and 390 cm^{-1} for diopside can still be observed on this spectrum (Fig. 5). This indicates that some diopside relicts are remained in this grain. Hence, we assume that this CaMgFe-silicate grain could be a shock-metamorphosed diopside that has broken down to some other silicate phases and glassy materials. It is this grain that draws our attention to conduct a detailed study on it.

3.2 Breakdown of the shock-metamorphosed diopside grain

3.2.1 Occurrence

The studied shock-metamorphosed diopside grain occurs in a shock melt vein of the Suizhou meteorite (Fig. 3). It has a rounded outline and grain size of 40 μm in diameter and closely associates with other two high-pressure minerals lingunite and ringwoodite. This multi-phase grain is embedded in the fine-grained vein matrix consisting of fine-grained majorite-pyrope$_{s.s.}$, magnesiowüstite and small eutectic FeNi-FeS blebs.

Our TEM and STEM studies revealed that this shock-metamorphosed diopside grain is not a mono-mineral phase but an aggregate of different CaMg-silicate phases (Fig. 6). This implies that this grain would have decomposed to several phases by shock. The identification of these phases by STEM, EDXS and Raman spectroscopy will be given in the next sections.

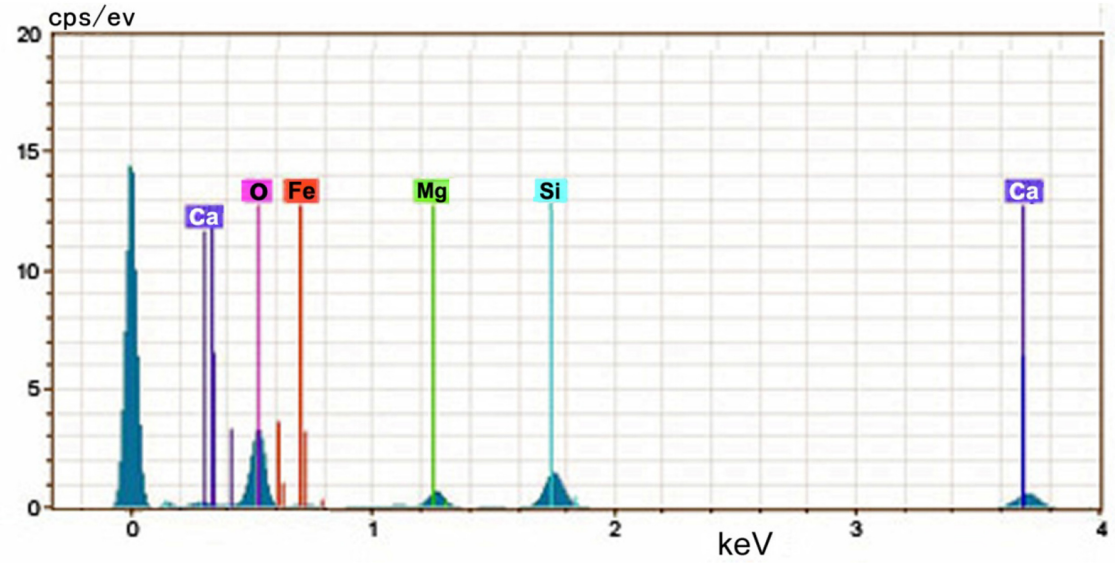

Fig. 4 EDXS diagram showing the presence of Mg. Ca, Fe, Si, and O in the shock-metamorphosed diopside grain

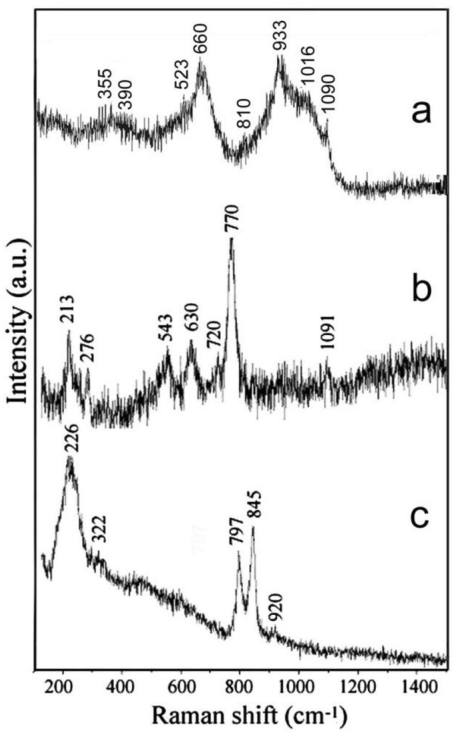

Fig. 5 Raman spectrum of the shock-metamorphosed diopside grain (**a**) coexisting with lingunite (**b**) and ringwoodite (**c**) in a shock melt vein of the Suizhou meteorite

3.2.2 *Chemical compositions*

The analysis of chemical compositions of diopside breakdown products was carried out by EDXS equipped with the FEI Talos F200s STEM. The results of analyses on 10 grains, from No.1 to No.10 marked in Fig. 6, are listed in Table 2. From this table, we can see that four silicate phases of different compositions in this shock-metamorphosed diopside grain are observed, namely, phase A, phase B, phase C, and phase D. We use the average element contents of each phase and the fixed number of oxygens per formula (O = 3) to calculate their chemical formulas and the results are listed below the table.

3.2.3 *Phase A—the orthorhombic $(Ca_{0.663}Mg_{0.314})SiO_3$-perovskite*

Phase A is the main breakdown product of diopside in the Suizhou meteorite upon shock. Figure 7 are the bright field, SAED, and high-resolution (HR) TEM images of this phase. Figure 7a and 7b show the close association of phase A with phase B. Phase A has a rounded shape and grey color with a smooth surface.

As it has been shown in Table 2, the chemical formula of phase A is $(Ca_{0.663}Mg_{0.314})_{0.977}(Si_{0.982}Al_{0.06})_{0.988}O_3$, and its simplified formula is $(Ca_{0.663}Mg_{0.314})SiO_3$, or even (Ca, Mg)$SiO_3$. Here the atom units of Ca in phase A is as twice larger than that of Mg, and phase A does not contain FeO (Table 2).

Based on the results of our TEM study (Fig. 7) and EDXS analyses (Table 2), we can identify that phase A (grain No. 1 in Fig. 6) is a crystalline silicate with $(Ca_{0.663}Mg_{0.314})SiO_3$ composition, for it gives electron diffraction spots and lattice fringes on its SAED and HRTEM images (Fig. 7c, e, and f), respectively.

For further identification of phase A, besides the HRTEM image and the SAED pattern taken from grain No.1 (Fig. 7e and f), we also obtained HRTEM images and related SAED patterns on another 4 phase A grains.

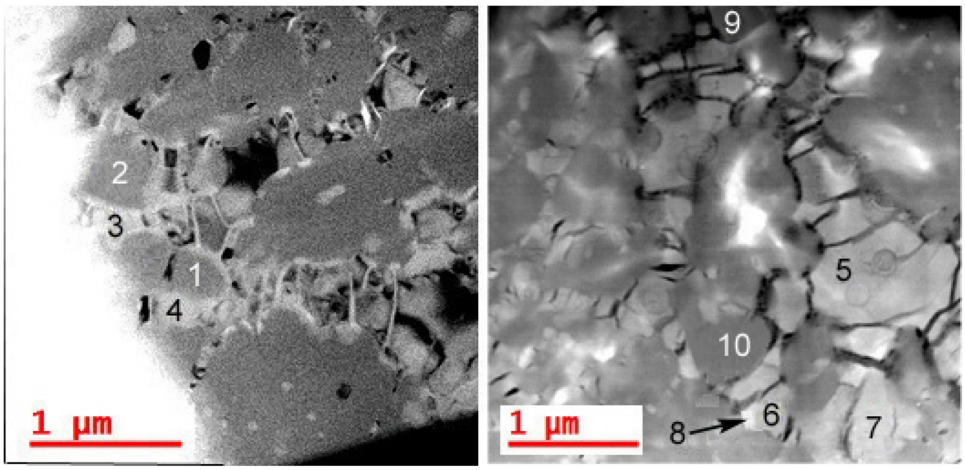

Fig. 6 STEM bright field images of the shock-metamorphosed diopside grain in a shock melt vein of the Suizhou meteorite. The numbers from 1 to 10 show the tiny grains of different phases contained in this diopside grain where the STEM study and EDXS analysis were conducted

Table 2 Chemical composition of diopside breakdown products in Suizhou meteorite (wt%)

Grain no.	Phase A			Phase B					Phase C			Phase D		
	1	2	Ave.	3	4	5	6	Ave.	7	8	Ave.	9	10	Ave.
SiO_2	53.93	54.10	54.02	51.83	51.37	55.87	55.50	53.64	57.83	56.48	57.16	55.29	54.58	54.94
TiO_2	–	–	–	0.06	–	–	0.35	0.10	–	0.32	0.16	–	–	–
FeO	–	–	–	8.81	8.86	4.99	3.25	6.48	–	–	–	–	–	–
MgO	14.09	11.71	12.95	25.29	23.20	23.74	23.33	23.89	33.35	31.55	32.45	23.53	19.88	21.71
CaO	31.33	34.20	32.77	8.12	10.12	14.35	17.09	12.41	7.72	9.68	8.70	19.44	23.77	21.61
Al_2O_3	0.56	–	0.28	3.72	3.84	–	0.48	2.01	0.51	1.35	0.93	0.98	0.95	0.97
Cr_2O_3	–	–	–	0.11	0.07	1.17	–	0.34	0.58	0.53	0.56	0.67	0.75	0.71
Na_2O	–	–	–	1.19	1.55	–	–	0.69	–	–	–	–	–	–
Total	99.91	100.07	99.42	99.13	99.01	100.12	100.00	99.56	99.99	99.91	99.96	99.91	99.93	99.95

Chemical formula: Phase A—$(Ca_{0.663}Mg_{0.314})_{0.977}(Si_{0.982}Al_{0.06})_{0.988}O_3$;

Phase B—$(Mg_{0.642}Ca_{0290}Fe_{0.098}Ti_{0.001}\ Na_{0.024}Cr_{0.005})_{1.060}(Si_{0.967}Al_{0.043})_{1.010}O_3$;

Phase C—$(Mg_{0.853}Ca_{0.167}Ti_{0.001}\ Na_{0.023}Cr_{0.004})_{1.048}(Si_{0.949}Al_{0.041})_{0.990}O_3$;

Phase D—$(Mg_{0.578}Ca_{0.414}Cr_{0.010})_{1.002}(Si_{0.981}Al_{0.020})_{1.001}O_3$

Figure 8 shows a representative HRTEM image and SAED pattern obtained from grain A4. The *d* spacing values of phase A measured from above mentioned 5 grains are listed in Table 3. In this table, grain No.1 in Table 2 is marked as A1.

The *d* spacing values of 5 phase A grains show the following characteristics: (1) All 5 grains gave very similar *d* spacing values in 2.671–2.690 Å (2.678 Å in average), 1.902–1.914 Å (1.909 Å in average), and 1.329–1.355 Å (1.339 Å in average). (2) The *d* spacing values measured for the strongest electron diffraction spots are 2.671–2.690 Å (2.678 Å on average). (3) The *d* spacing values measured for the less strong electron diffraction spots are 1.902–1.914 Å (1.909 Å in average) and 1.329–1.355 Å (1.339 Å on average).

The obtained *d* spacing values and cell parameters (a = 5.358 Å, b = 7.636 Å, c = 5.400 Å, V = 222.934 Å^3) for phase A can be compared with those of orthorhombic $CaTiO_3$-perovskite (PDF 72·1192) (Table 4), and are close to those of the new high-pressure mineral hiroseite, the Fe-rich analog of bridgmanite with orthorhombic perovskite structure and $(Fe_{0.54}Mg_{0.37}Na_{0.03}Ca_{0.02})(Si_{0.89}Al_{0.15})O_3$ composition discovered in a shock vein of the same Suizhou meteorite (Bindi et al. 2020). Hence, we identify phase A in the Suizhou shock-metamorphosed diopside as orthorhombic $(Ca_{0.663}Mg_{0.314})SiO_3$-perovskite.

3.2.4 *Phase B—the vitrified $(Mg_{0.642}Ca_{0.290}Fe_{0.098})SiO_3$ perovskite*

Phase B is also a main breakdown product of the shock-metamorphosed diopside in the Suizhou melt vein. Figure 7 shows the bright field, SAED, and high-resolution (HR) TEM images of this phase. Figure 7a and b demonstrate its occurrence and close association with phase A. Phase B is of irregular or ladder shape and light color, and

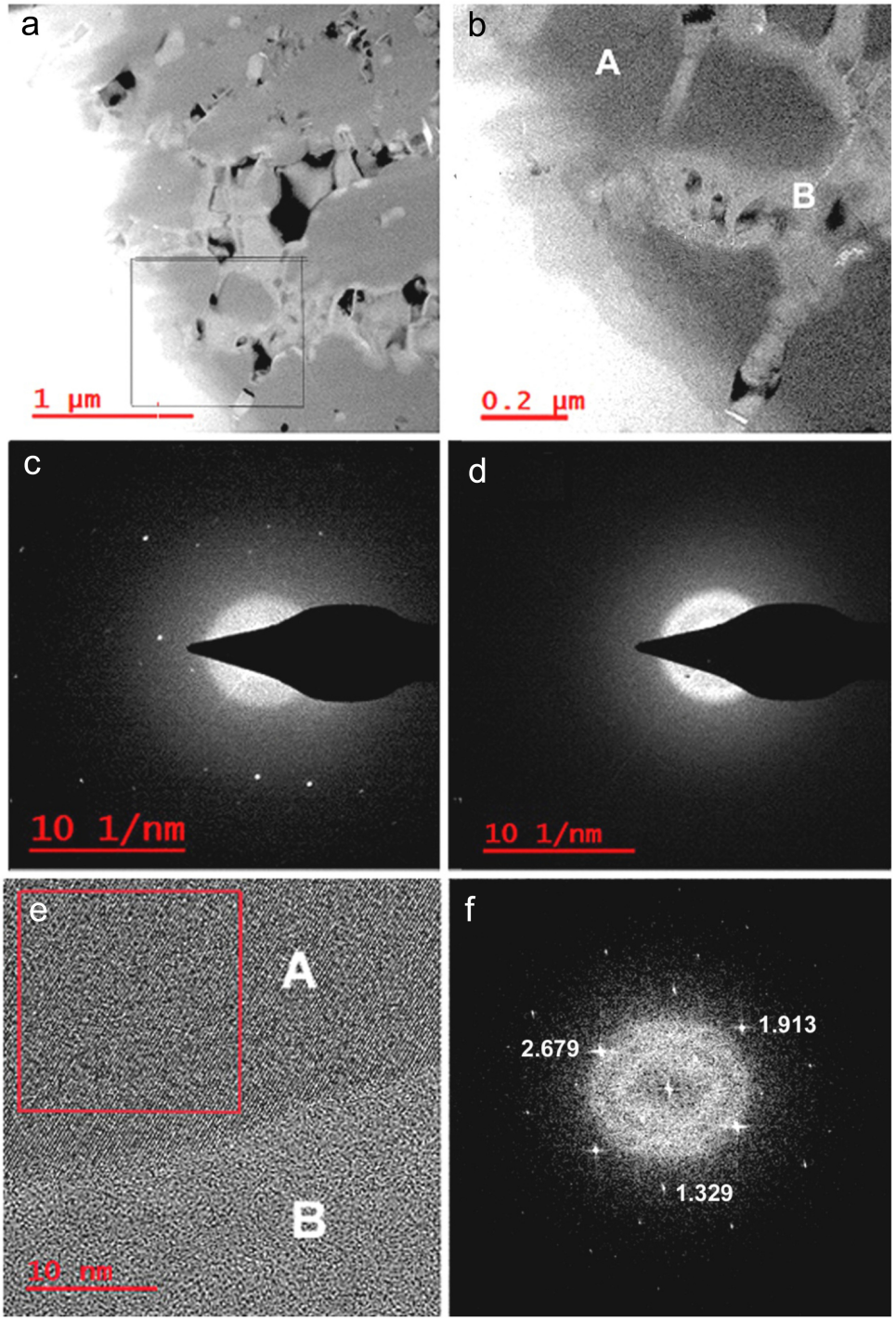

Fig. 7 TEM images showing the breakdown of a diopside grain to phase A (grain No. 1 in Fig. 6) and Phase B (grain No. 4 in Fig. 6). **a** Bright-field image of a shock-metamorphosed diopside grain. **b** Enlarged image from the frame area of 7**a** showing the occurrence of phase A and phase B. **c** SAED pattern taken from phase A. **d** SAED pattern taken from phase B. **e** HRTEM image showing the crystalline phase A and glassy phase B. **f** SAED pattern taken from the frame area of phase A

occurs around or in the interstices of phase A grains. Because of the volume shrinkage during cooling and solidification, some fractures/cracks crosscutting the phase B grains are observed (Fig. 6, grains 3, 4, 5, and 6).

As it has been shown in Table 2, the chemical formula of phase B is $(Mg_{0.642}Ca_{0290}Fe_{0.098}Ti_{0.001}Na_{0.024}Cr_{0.005})_{1.060}(Si_{0.967}Al_{0.043})_{1.010}O_3$; and its simplified formula is $(Mg_{0.642}Ca_{0.290}Fe_{0.098})SiO_3$, or (Mg, Ca, Fe)$SiO_3$. It must be pointed out that FeO is always present in phase B (Table 2), and the FeO content (6.48 wt%) in phase B is a litter higher than that in the un-metamorphosed diopside (5.40–5.71 wt%) occurred in the Suizhou chondritic rock (Table 1).

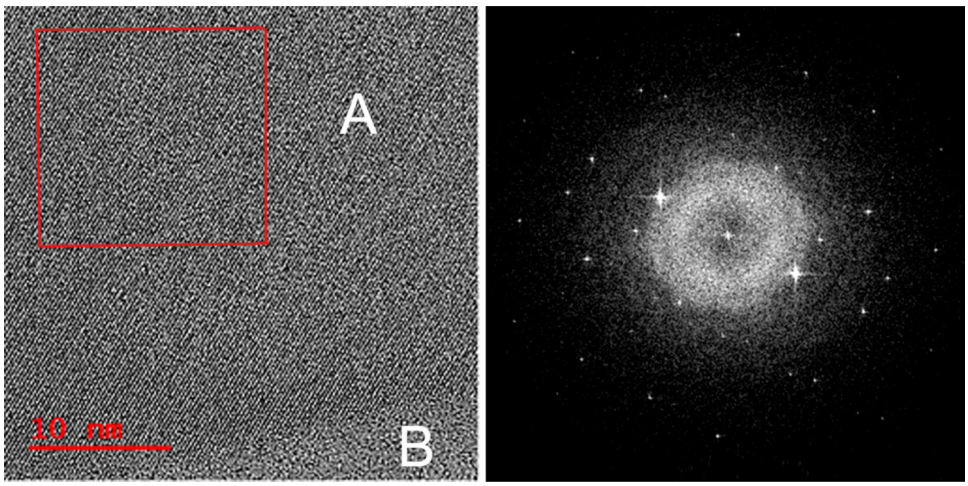

Fig. 8 The HRTEM image of grain A4 (Left, see Table 3) and the SAED pattern taken from the frame area (Right). A = phase A, B = phase B

Table 3 The *d* spacing of phase A measured from SAED patterns (Å)

Grains	A.1	A2	A3	A4	A5	Average	Intensity
1	**2.679**	**2.671**	**2.690**	**2.671**	**2.679**	**2.678**	**VS**
2	2.133	2.127	2.133	2.127		2.130	W
3	**1.913**	**1.914**	**1.903**	**1.912**	**1.902**	**1.909**	**S**
4	1.492	1.489		1.490		1.490	W
5	**1.329**	**1.355**	**1.336**	**1.334**	**1.342**	**1.339**	**M**
6		1.283	1.289	1.287	1.285	1.286	W
7					1.196	1.196	W
8				1.087	1.103	1.095	W
9				1.063		1.063	W
10				1.019	1.018	1.019	W
11				0.958		0.958	W
12				**0.911**		**0.911**	W
13					0.896	0.896	W

The main d values are shown in bold

Table 4 Comparison of electron diffraction data of Ca-perovskite in Suizhou meteorite with standard orthorhombic $CaTiO_3$-perovskite

$CaSiO_3$-perovskite in Suizhou			$CaTiO_3$-perovskite (PDF 72·1192)		
hkl	*d*	*I**	*hkl*	*d*	*I*
200	2.678	VS	121	2.7025	999
			200	2.6835	272
040	1.909	S	040	1.9109	669
			321	1.5529	181
220	1.339	M	220	1.3512	166
310	1.196	M	310	1.2085	78
Orthorhombic,			Orthorhombic,		
a = 5.358 Å, b = 7.636 Å,			a = 5.367 Å, b = 7.643 Å,		
c = 5.400 Å, V = 222.934 Å^3			c = 5.443 Å, V = 223.272 Å^3		

*VS = very strong, S = strong, M = moderate

Interestingly, the chemical composition of phase B and phase A are complementary with each other in Mg and Ca. The atom units of Mg and Ca for phase A almost equal to those of Ca and Mg for phase B (Table 2). This future can also be seen on STEM element maps of these two phases (Fig. 9), where the Mg-rich and Fe-bearing phase B occurs in between two Ca-rich phase A grains. Hence, we assume that both phase B and phase A are the main decomposition products of diopside with $(Ca_{0.435}\ Mg_{0.449}Fe_{0.084})SiO_3$ composition in the Suizhou meteorite.

Based on the results of our TEM study (Fig. 7) and EDXS analyses (Table 2), we could identify that phase B is a silicate glass with $(Mg_{0.642}Ca_{0.290}Fe_{0.098})SiO_3$ composition, for it does not give any electron diffraction spots and lattice fringes on its SAED and HRTEM images, respectively (Fig. 7d and e).

Chen et al (2004a) reported the finding of a unique occurrence of fine-grained shock-produced (Mg, Fe)SiO_3 glass that intimately coexisted with majorite in the shock veins of the Suizhou meteorite. They indicated that this (Mg, Fe)SiO_3 glass is the vitrified product of (Mg, Fe)SiO_3 perovskite after pressure release at post-shock temperature. They also indicated that the heating experiments and the molecular- and lattice dynamics calculations indicated that the crystalline $MgSiO_3$ perovskite would be decompressed to an amorphous phase near the ambient pressure from its high-pressure stability fields at modest temperatures (Durben and Wolf 1992; Hemmati et al. 1995). The vitrification of $MgSiO_3$ perovskite begins above 127 °C and is complete by 477 °C at ambient pressure (Durben and Wolf 1992). The post-shock temperature must have been higher than 477 °C inducing a rapid vitrification of crystalline $MgSiO_3$ perovskite.

Our phase B is a shock-produced Ca-rich and Fe-bearing $MgSiO_3$ glass with $(Mg_{0.642}Ca_{0.290}Fe_{0.098})SiO_3$ composition, it would have similar behavior with the shock-produced (Mg, Fe)SiO_3 glass reported by Chen et al (2004a) in

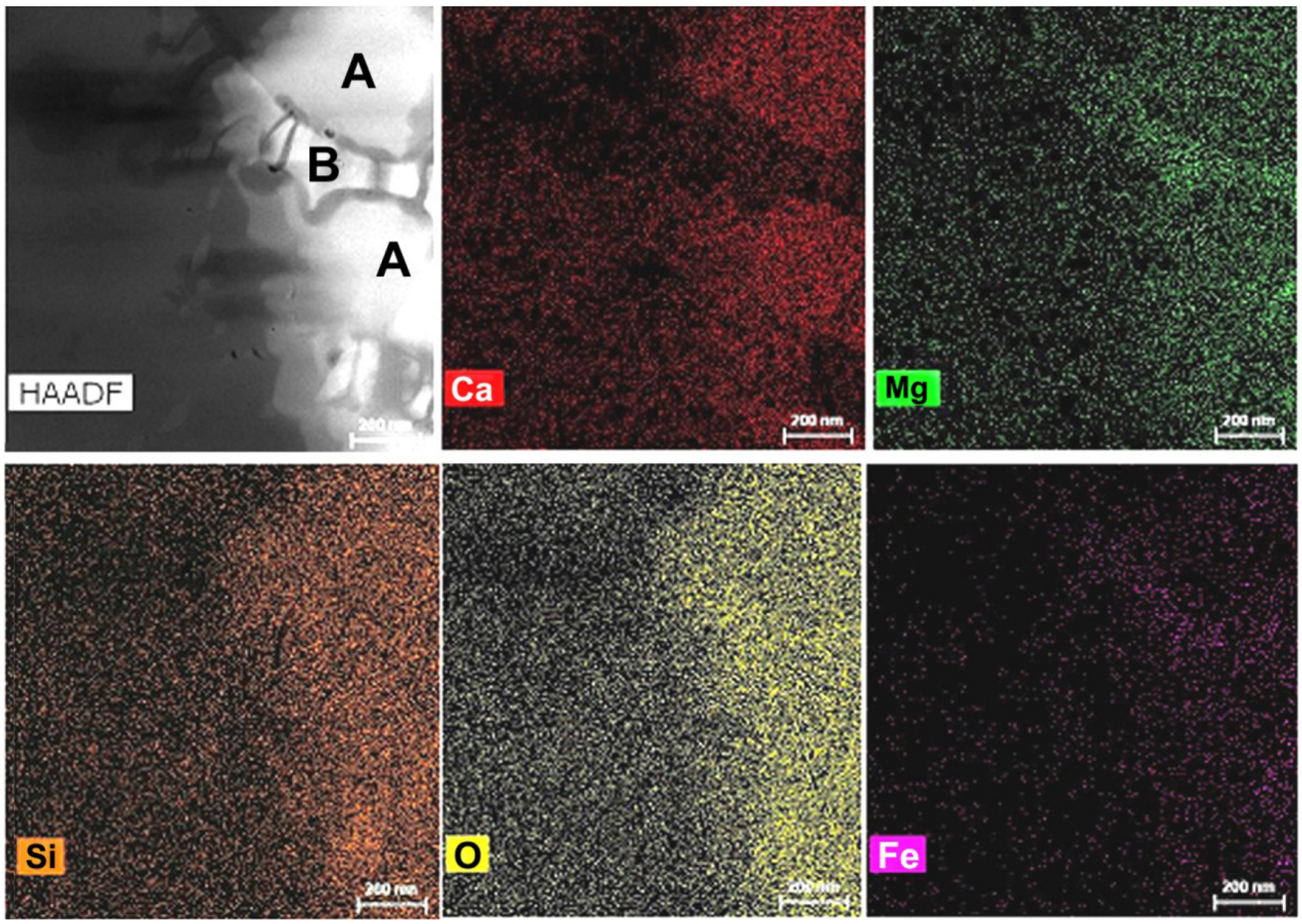

Fig. 9 STEM element maps of phase B and phase A in the shock-metamorphosed diopside grain. The Mg-rich and Fe–bearing phase B occur in between two Ca-rich phase A grains

the shock veins of the same Suizhou meteorite after pressure release at post-shock temperature. Hence, we assume that the glassy phase B would be the vitrified (Mg, Ca, Fe)SiO_3 perovskite.

3.2.5 *Phase C—the verified Ca-rich ($Mg_{0.853}Ca_{0.167}$)SiO_3 perovskite*

Phase C is the third breakdown product of the shock-metamorphosed diopside in the Suizhou meteorite (Fig. 6, grains 7 and 8). It has an irregular shape and light grey color. Some volume shrinkage-produced fractures/cracks crosscutting the phase C grains are also observed. The chemical formula of phase C is $(Mg_{0.853}Ca_{0.167}Ti_{0.001}Na_{0.023}Cr_{0.004})_{1.048}(Si_{0.949}Al_{0.041})_{0.990}O_3$ (Table 2), and its simplified formula is $(Mg_{0.853}Ca_{0.167})SiO_3$, or (Mg, Ca)$SiO_3$. Although the atom units of Mg in phase C is as 5 times larger than that of Ca, but the Ca content is still rich enough (CaO = 8.70 wt%), and phase C does not contain FeO (Table 2).

The Raman spectrum of phase C only shows two wide brands at 660 and 971 cm^{-1} (Fig. 10a), indicating that phase C in the Suizhou shock-metamorphosed diopside is a silicate glass. The Raman spectrum of phase C can be compared with that of the shock-produced $(Mg_{0.759}Fe_{0.202}Ca_{0.014})SiO_3$ glass, the verified perovskite, in a melt vein of the same Suizhou meteorite reported by Chen et al. in 2004a (Fig. 10b). Hence, we identify that phase C in the Suizhou shock-metamorphosed diopside is a vitrified Ca-rich Mg-perovskite with $(Mg_{0.853}Ca_{0.167})SiO_3$ composition.

3.2.6 *Phase D—the Mg–Ca majorite with ($Mg_{0.578}Ca_{0.414}$)SiO_3 composition*

Phase D is the fourth breakdown product of the shock-metamorphosed diopside in the Suizhou meteorite (Fig. 6, grains 9 and 10). It has an irregular or granular shape and dark grey color. Phase D grains are commonly surrounded by glassy phase C. The chemical formula of phase D is $(Mg_{0.578}Ca_{0.414}\ Cr_{0.010})_{1.002}(Si_{0.981}Al_{0.020})_{1.001}O_3$ (Table 2), and its simplified formula is $(Mg_{0.578}Ca_{0.414})SiO_3$, or (Mg, Ca)$SiO_3$. Here we can see that the atom unit of Mg in phase D is just a litter larger than that of Ca, and phase D does not contain FeO (Table 2).

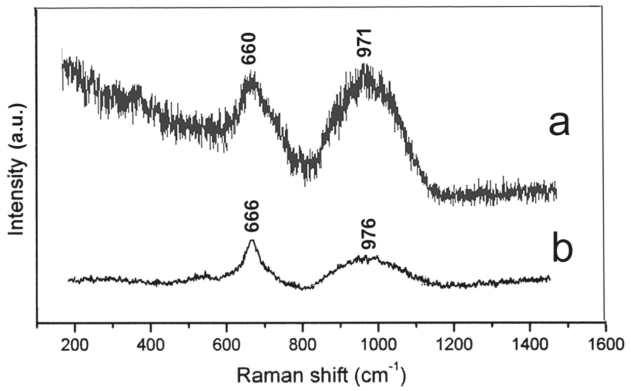

Fig. 10 **a** Raman spectrum of phase C in the Suizhou shock-metamorphosed diopside grain. **b** Raman spectrum of $(Mg_{0.759}Fe_{0.202}Ca_{0.014})SiO_3$ glass in a Suizhou shock melt vein (Chen et al. 2004a)

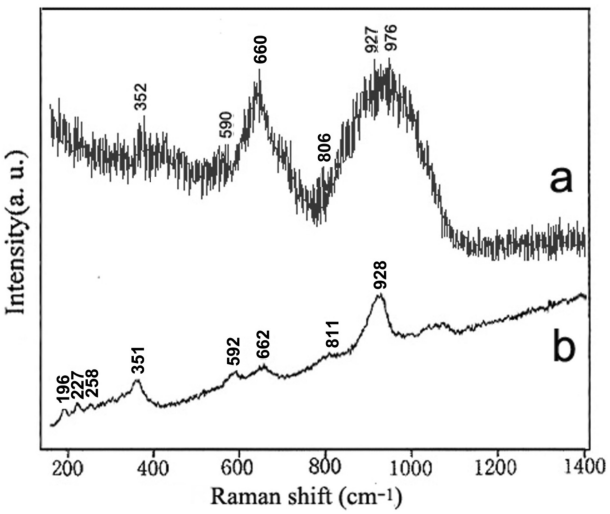

Fig. 11 **a** Raman spectrum of phase D + glassy phase C in the shock-metamorphosed diopside grain. **b** Raman spectrum of majorite in a Suizhou shock melt vein (Xie et al. 2001a)

The Raman spectrum of the phase D grain surrounded by glassy phase C in the Suizhou shock-metamorphosed diopside grain shows Raman peaks at 976, 927, 806, 660, 590, and 352 cm^{-1} (Fig. 11a). The two wide brands at 976 and 660 cm^{-1} can be assigned to the coexisting glassy phase C (see Fig. 10a), and the peaks at 927, 806, 660, 590, and 352 cm^{-1} can be compared with that of majorite, the (Mg, Fe)SiO_3-garnet, in a Suizhou melt vein reported by Xie et al. in 2001a (Fig. 11b). Hence, we assume that phase D in the Suizhou shock-metamorphosed diopside is (Mg, Ca)SiO_3 majorite with $(Mg_{0.578}Ca_{0.414})SiO_3$, composition.

4 Discussion

4.1 The coexisting of orthorhombic crystalline Ca-perovskite and vitrified

4.1.1 Ca-rich and Fe-bearing Mg-perovskite

As we know that a series of experimental studies on the phase relations of diopside $CaMgSi_2O_6$ under high pressures and high temperatures have been performed. The most pioneering experiments on phase transformations in diopside were performed by Mao et al. (1977) using a diamond anvil cell and laser heating techniques, and samples were quenched from 21.7 and 42.1 GPa. Their results show that, under pressure, the diopside had disproportionated into two perovskite phases, with chemical compositions close to $CaSiO_3$ and $MgSiO_3$.

Tamai and Yagi (1989) then conducted the study of phase transformation of synthetic $CaMgSi_2O_6$ single crystal up to 50 GPa. They indicated that $CaMgSi_2O_6$ was also found to break down into $CaSiO_3$ perovskite and $MgSiO_3$ perovskite. Kim et al. (1994) also carried out a phase transformation study on natural crystalline diopside at a pressure of up to 34.5 and 30 GPa, respectively, and at $\sim$ 1000 °C. They found that the crystalline diopside breaks down to cubic $CaSiO_3$ perovskite and orthorhombic $MgSiO_3$ perovskite. Oguri et al. (1997) studied phase transformations in diopside $Ca_{0.92}Mg_{1.08}Si_2O_6$ at pressures of 18–24 GPa and temperatures of 1000–2400 K. Their results show that diopside transformed into (Mg, Ca)SiO_3 garnet and $CaSiO_3$ perovskite, and then to $MgSiO_3$-perovskite and $CaSiO_3$-perovskite. Irifiune et al. (2000) performed experiments on high-pressure phase transformation in diopside $CaMgSi_2O_6$ at pressures 23–27 GPa and temperatures 1000–1900 °C. They found that all run products consisted of $MgSiO_3$-rich orthorhombic perovskite and amorphous $CaSiO_3$, the latter having been converted from cubic perovskite.

To sum up, the results of all above-listed experiments performed on diopside $CaMgSi_2O_6$ at pressures range of 18–50 GPa are very similar: the diopside had finely broken down into cubic $CaSiO_3$–perovskite and orthorhombic $MgSiO_3$–perovskite, and one of the intermediate products is (Mg, Ca)SiO_3 garnet (Ca-rich Mg-majorite).

The natural (Mg, Fe)SiO_3 perovskite, as the high-pressure mineral that partially replaced strongly deformed pyroxene, was found by Tomioka and Fujino (1997) in the shock veins of the Tenham (L6) chondrite. The natural cubic $CaSiO_3$-perovskite (daveomaoite) was found as inclusion in a diamond from Orapa kimberlite, Botswana (Tschauner et al. 2021). However, No crystalline Ca-perovskite was found in any shocked meteorites before (Chen et al. 2004a; Xie and Chen 2016; Martinez et al. 2019).

The natural crystalline Mg-rich Ca-perovskite with $(Ca_{0.663}Mg_{0.314})SiO_3$ composition (phase A) now is found for the first time in a shock-metamorphosed diopside grain of the Suizhou L6 chondrite. This crystalline Ca-perovskite

is closely associated with vitrified Ca-rich and Fe-bearing Mg-perovskite with $(Mg_{0.642}Ca_{0.290}Fe_{0.098})SiO_3$ composition (phase B). Both phases constitute the main products of diopside breakdown in the Suizhou melt vein. Although the breakdown products of natural diopside in Suizhou chondrite are consistent with those obtained by high-pressure and high-temperature experiments, we could still observe some differences between them: (1) our crystalline Mg-rich Ca-perovskite belongs to an orthorhombic system that is different with the cubic davemaoite and cubic crystalline Ca-perovskite experimentally obtained using diopside as the starting material. The reason for this is still unknown, but it may be related to the different *P–T* history between natural and experimental phase transition processes. (2) our Ca-rich and Fe-bearing Mg-perovskite have been vitrified after pressure release at post-shock temperature, while the experimentally obtained $MgSiO_3$ perovskite is the crystalline phase after rapid annealing. (3) our vitrified Ca-rich Mg-perovskite contains 6.48 wt% of FeO (Table 2) indicating that the Fe-bearing diopside (FeO = 5.40–5.71 wt%) in the Suizhou chondritic rock shifted its total Fe into vitrified Mg-perovskite during its breakdown upon shock, whereas the experimentally obtained $MgSiO_3$ perovskite does not, for its starting material is Fe-free diopside.

4.2 The coexisting of $(Mg_{0.578}Ca_{0.414})SiO_3$ majorite with vitrified Ca-rich Mg-perovskite with $(Mg_{0.853}Ca_{0.167})SiO_3$ composition

Natural $(Mg,Fe)SiO_3$ majorite has been found in melt veins of many shocked L6 chondrites (Coleman 1977; Xie et al. 2001a; Chen et al. 2004a). Natural Ca-rich Mg-majorite, as the breakdown product of diopside, was first reported in the Shergotty Martian meteorite (Malavergne et al. 2001). Then Ca-rich Mg-majorite has also been found in two ordinary chondrites: Yamato 75,100 (H6) (Tomioka and Kimura 2003) and Tenham (L6) (Xie and Sharp 2007). The Ca-rich Mg-majorite ($En_{65}Fs_9Wo_{26}$) in Yamato 75,100 has a granular texture and is associated with a Ca-rich glass ($En_{23}Fs_5Wo_{72}$), whereas in Tenham, Ca-rich Mg-majorite ($En_{64}Fs_{10}Wo_{27}$) occurs as a nanometer symplectic intergrowth with amorphous Ca-bearing glass (Xie and Sharp 2007). More recently, Martinez et al. (2019) reported the third finding of Ca-rich ($En_{47}Fs_7Wo_{45}$) Mg-majorite together with Ca-poor ($En_{77}Fs_{21}Wo_2$) Mg-majorite in the melt veins of the Villalbeto de la Pena (L6) chondrite. Their electron microprobe analyses and Raman spectra show that original low-Ca pyroxene, high-Ca pyroxene, olivine, and plagioclase in the shock vein are transformed into their high-pressure polymorphs, low-Ca Mg-majorite, high-Ca Mg-majorite, ringwoodite, and a mixture of jadeite-lingunite, respectively. Chen et al (2004a) reported the finding of the majorite with $(Mg_{0.761}Fe_{0.202}Ca_{0.015})SiO_3$ composition that intimately coexisted with vitrified perovskite with $(Mg_{0.759}Fe_{0.202}Ca_{0.014})SiO_3$ composition in shock veins of the Suizhou meteorite.

In the Suizhou shock-metamorphosed diopside grain, we observed MgCa-majorite with $(Mg_{0.578}Ca_{0.414})SiO_3$ composition (phase D) that coexisted with vitrified Ca-rich Mg-perovskite with $(Mg_{0.853}Ca_{0.167})SiO_3$ composition (phase C). This assemblage is similar to that in the Yamato 75,100 (H6) chondrite, where the Ca-rich Mg-majorite ($En_{65}Fs_9Wo_{26}$) is associated with a Ca-rich silicate glass ($En_{23}Fs_5Wo_{72}$). Our Suizhou MgCa-majorite is also very similar to the Ca-rich ($En_{47}Fs_7Wo_{45}$) Mg-majorite in the melt veins of the Villalbeto de la Pena (L6) chondrite (Martinez et al. 2019). Furthermore, one of the intermediate products experimentally obtained on the diopside is $(Mg,Ca)SiO_3$ majorite, (Oguri et al. 1997). Therefore, we assume that the MgCa-majorite associated with vitrified Ca-rich Mg-perovskite in the Suizhou meteorite might also be the common product formed by decomposition of the shock-metamorphosed diopside.

4.3 The *P–T* history of diopside decomposition in the Suizhou melt vein

High-pressure experiments indicated that $MgSiO_3$ crystallizes in perovskite structures above 23 GPa and at ~2000 °C (Liu 1974, 1975; Gasparik 1996; Chen et al. 2004b), and that $MgSiO_3$ majorite has a P–T stability field between 16 and 22.5 GPa and 1600–2500 °C (Gasparik 1996; Presnall 2000; Chen et al. 2004b). The crystalline $MgSiO_3$ perovskite would be decompressed to an amorphous phase near the ambient pressure from its high-pressure stability fields at temperatures higher than 477 °C (Durben and Wolf 1992; Hemmati et al. 1995). Quench experiments have confirmed the decomposition of diopside in a wide temperature range of 1000–1900 °C and at pressures 23–27 GPa (Irifune et al. 2000).

The pressure and temperature history in the shock veins of meteorites can be well-constrained by high-pressure mineral assemblage (Agee et al. 1995; Chen et al. 1996; Xie and Chen 2016, 2020). For instance, on the bases of the high-pressure mineral assemblage of Ca-rich Mg-majorite, Ca-poor Mg-majorite, ringwwodite, jadeite-lingunite, and magnesiowüstite in the melt veins of the Villalbeto de la Pena (L6) chondrite, the *P–T* conditions of between 16 and 28 GPa and 2000–2200 °C were estimated (Martinez et al. 2019).

The assemblage of ringwoodite, majorite, lingunite, and magnesiowüstite in the shock veins of the Suizhou meteorite should have crystallized at pressures of 20–22 GPa and temperatures of 1800–2000 °C (Chen et al. 1996; Xie et al. 2001a), however, the recent discovery of hiroseite, the Fe-rich analog of perovskite–structured bridgmanite, in

a Suizhou melt vein, raised its *P–T* conditions up to 24 GPa and > 2000 °C (Bindi et al. 2020; Agee et al. 1995). Hence, we conclude that the diopside-containing melt vein in the Suizhou meteorite would have experienced a high-pressure and high-temperature regime of 20–24 GPa and 1800–>2000 °C. This high enough *P–T* regime is satisfied for the decomposition of diopside, as well as for the formation of crystalline orthorhombic $(Ca_{0.663}Mg_{0.314})SiO_3$-perovskite (phase A), Ca-rich and Fe-bearing Mg-perovskite with $(Mg_{0.642}Ca_{0.290}Fe_{0.098})$ composition (phase B), and Ca-rich and Fe-free Mg-perovskite with $(Mg_{0.853}Ca_{0.167})$-SiO_3 composition (phase C). Both phase B and Phase C then turned to amorphous phases after pressure release and upon cooling, while phase A is remained stable. This is because the high-pressure experiments on the dioipside revealed that decomposed $CaSiO_3$ is stable at pressure release, but the crystalline $MgSiO_3$ perovskite would be decompressed to an amorphous phase near the ambient pressure from its high-pressure stability fields at temperatures higher than 477 °C (Durben and Wolf 1992; Hemmati et al. 1995). As for the $(Mg_{0.578}Ca_{0.414})SiO_3$ majorite (phase D), it would be formed at 16–22.5 GPa and 1600–2500 °C (Gasparik 1996; Presnall 2000; Chen et al. 2004b). This *P–T* condition is lower than that for Ca- and Mg-perovskites, but is within the *P–T* regime that the Suizhou melt vein experienced.

As we know, davemaoite, the natural cubic $CaSiO_3$-perovskite, is the high-pressure silicate recovered from the lower mantle in 2021 (Tschauner et al. 2021), and bridgmanite, another lower-mantle mineral, was found inside a melt vein of the Tenham L6 chondrite in 2014 (Tschauner et al. 2014). Both formed an exclusive club as the only lower-mantle silicate minerals confirmed in nature. But, our orthorhombic $(Ca_{0.663}Mg_{0.314})SiO_3$ perovskite found in the Suizhou L6 chondrite might serve as the third lower-mantle silicate mineral, a new member of this exclusive club after its crystal structure and physical property analyses being completed.

5 Conclusion

(1) The Suizhou L6 chondrite contains a minor amount of diopside with $(Ca_{0.419}\ Mg_{\ 0.466}Fe_{0.088})SiO_3$ composition, and a unique shock-metamorphosed diopside grain associated with lingunite and ringwoodite was found in a shock melt vein of the Suizhou meteorite.

(2) Four silicate phases of different composition and structures in this shock-metamorphosed diopside grain are observed, namely, phase A, phase B, phase C and phase D.

(3) Phase A is identified as orthorhombic $(Ca_{0.663}Mg_{0.314})SiO_3$-perovskite which is closely associated with phase B, the vitrified $(Mg_{0.642}Ca_{0.290}Fe_{0.098})$-$SiO_3$ perovskite. The chemical composition of phase A and phase B are complementary with each other in Ca and Mg.

(4) Phase D is assigned to be Ca-rich $(Mg_{0.578}Ca_{0.414})$-SiO_3-majorite which is associated with phase C, the verified Ca-rich Mg-perovskite with $(Mg_{0.853}Ca_{0.167})SiO_3$.composition.

(5) The diopside-containing melt vein in the Suizhou meteorite would have experienced a high-pressure and high-temperature regime of 20–24 GPa and 1800– > 2000 °C. This *P–T* regime is high enough for the decomposition of the diopside and the formation of different silicate phases.

(6) After the crystal structure and physical property analyses are **completed** the orthorhombic $(Ca_{0.663}Mg_{0.314})SiO_3$ perovskite found in the Suizhou L6 chondrite might serve as the third lower-mantle silicate mineral after bridgmanite and davemaoite.

Declarations

Conflict of interest We declare no conflict of interest in this study. The manuscript has not been submitted to more than one journal for simultaneous consideration.

References

Agee CB, Li J, Shannon MC, Circone S (1995) Pressure temperature phase diagram for the Allende meteorite. J Geophys Res 100:17725–17740

Bindi L, Chen M, Xie XD (2017) Discovery of the Fe-analogue of akimotoite in the shocked Suizhou L6 chondrite. Sci Rep 7:42674

Bindi L, Brenker FE, Nestola F, Koch TE, Prior DJ, Lilly K, Krot AN, Bizzarro M, Xie XD (2019) Discovery of asimowite, the Fe-analog of wadsleyite, in shock-melted silicate droplets of the Suizhou L6 and the Quebrada Chimborazo 001 CB3.0 chondrites. Am Miner 104:775–778

Bindi L, Shim SH, Sharp TG, Xie XD (2020) Evidence for the charge disproportionation of iron in extraterrestrial bridgmanite. Sci Adv 6:eaay7893

Bindi L, Sinmyo R, Bykova E, Ovsyannikov SV, McCammon C, Kupenko I, Ismailova L, Dubrovinsky L, Xie XD (2021) Discovery of elgoresyite, $(Mg, Fe)_5Si_2O_9$: implications for novel iron-magnesium silicates in rocky planetary interiors. ACS Earth Space Chem 5:2024–2130

Brearley AJ, Jones RH (1998) Chondritic meteorites. In: Papike JJ (ed) Planetary materials. Mineralogical Society of America, Washington DC

Chen M, Xie XD (2015) Shock-produced akimotoite in the Suizhou L6 chondrite. Sci China Earth Sci 58:876–880

Chen M, Sharp TG, El Goresy A, Wopenka B, Xie X (1996) The majorite-pyrope + magnesiowüstite assemblage: constraints on the history of shock veins in chondrites. Science

271(5255):1570–1573. https://doi.org/10.1126/science.271.5255.1570

Chen M, Shu JF, Xie XD, Mao HK (2003) Natural $CaTi_2O_4$-structured $FeCr_2O_4$ polymorph in the Suizhou meteorite and its significance in mantle mineralogy. Geochim Cosmochim Acta 67:3937–3942

Chen M, Xie XD, Goresy A (2004a) A shock-produced (Mg, Fe)SiO_3 glass in the Suizhou meteorite. Meteorit Planet Sci 39:1797–1808

Chen M, El Goresy A, Frost D, Gillet P (2004b) Melting experiments of a chondritic meteorite between 16 and 25 GPa: Implication for Na/K fractionation in a primitive chondritic Earth's mantle. Eur J Mineral 16:203–211

Chen M, Shu JF, Mao HK (2008) Xieite, a new mineral of high-pressure $FeCr_2O_4$ polymorph. Chin Sci Bull 53:3341–3345

Coleman LC (1977) Ringwoodite and majorite in the Catherwood meteorite. Can Mineral 15:97–101

Durben DJ, Wolf G (1992) High-temperature behavior of metastable $MgSiO_3$ perovskite: a Raman spectroscopic study. Am Miner 77:890–893

Gasparik T (1996) Melting experiments on the enstatite-diopside join at 70–224 kbar, including the melting of diopside. Contrib Mineral Petrol 124:139–153

Hemmati M, Chizmeshya A, Wolf GH, Poole PH, Shao J, Angell CA (1995) Cryst-Amorphous Trans Silicate Perovskites Phys Rev B 51:14841–14848

Irifune T, Miyashita M, Inoue T, Ando J, Funakoshi K, Utsumi W (2000) High-pressure phase transformation in $CaMgSi_2O_6$ and implications for origin of ultra-deep diamond inclusions. Geophys Res Lett 27:3541–3544

Kim YH, Li CM, Manghnani MH (1994) High-pressure phase transformations in a natural crystalline diopside and a synthetic $CaMgSi_2O_6$ glass. Phys Earth Planet Inter 83:61–79

Kubicki JD, Hemley RJ, Hofmeister AM (1992) Raman and infrared study of pressure-induced structuralchanges in $MgSiO_3$, $CaMgSi_2O_6$, and $CaSiO_3$ glasses. Am Miner 77:258–269

Liu LG (1974) Silicate perovskite from phase transformations of pyrope-garnet at high-pressure and temperature. Geophys Res Lett 1:277–280

Liu LG (1975) Post-oxide phases of forsterite and enstatite. Geophys Res Lett 2:417–419

Liu L (1987) New silicate perovskites. Geophys Res Lett 14:1079–1082

Ma C, Tschauner O, Beckett JR, Liu Y, Greenberg E, Prakapenka VB (2019) Chenmingite, $FeCr_2O_4$ in the $CaFe_2O_4$-type structure, a shock-induced, high-pressure mineral in the Tissint martian meteorite. Am Mineral 104:1522–1525

Malavergne V, Guyot F, Benzerara K, Martinez I (2001) Description of new shock-induced phases in the Shergotty, Zagami, Nakhla, and Chassigny meteorites. Meteorit Planet Sci 36:1297–1305

Mao HK, Yagi T, Bell PM (1977) Mineralogy of the earth deep mantle: quenching experiments on mineral composition at high pressure and temperature. Carnegie Institution of Washington, Washington, pp 502–504

Martinez M, Brearley AJ, Trigo-Rodríguez JM, Llorca J (2019) New observations on high-pressure phases in a shock melt vein in the Villalbeto de la Peña meteorite: insights into the shock behavior of diopside. Meteorit Planet Sci 54:2845–2863

Oguri K, Funamori N, Skai F, Kondo T, Uchida T, Yagi T (1997) High-pressure and high-temperature phase relations in diopside $CaMgSi_2O_6$. Phys Earth Planet Inter 104:363–370

Presnall DC (2000) Phase diagrams of earth-forming minerals. In: Ahrens TJ (ed) Mineral physics and crystallography. American Geophysical Union, Washington DC, pp 248–268

Tamai H, Yagi T (1989) High-pressure and high temperature phase relation in $CaSiO_3$ and $CaMgSi_2O_6$ and elasticity of perovskite-type $CaSiO_3$. Phys Earth Planet Inter 54:370–377

Tomioka H, Fujino K (1997) Natural (Mg, Fe)SiO_3 ilmenite and perovskite in the Tenham meteorite. Science 277:1084–1086

Tomioka N, Kimura M (2003) The breakdown of diopside to Ca-rich majorite and glass in shocked H chondrite. Earth Planet Sci Lett 208:271–278

Tomioka N, Bindi L, Okuchi T, Miyahara M, Iitaka T, Li Z, Kawatsu T, Xie XD, Purevjav N, Tani R, Kodama Y (2021) Poirierite, a dense metastable polymorph magnesium iron silicate in shocked meteorites. Nat Commun Earth Environ 2:16

Tschauner O, Ma C, Beckett JR, Prescher C, Prakapenka VB, Rossman GR (2014) Discovery of *bridgmanite,* the most abundant mineral in Earth, in a shocked meteorite. Science 346:1100–1102

Tschauner O, Huang S, Yang S, Humayun M, Liu W, Gilbert Corder SN, Bechtel HA, Tischler J, Rossman JR (2021) Davemaoite – $CaSiO_3$-perovskite as a mineral from the lower mantle. Nature 374:891–894

Xie XD, Chen M (2016) Suizhou meteorite: mineralogy and shock metamorphism. Springer-Verlag Berlin Heidelberg and Guangdong Science and Technology Press, Guangzhou, p 258

Xie XD, Chen M (2020) Yanzhuang meteorite: mineralogy and shock metamorphism. Springer-Verlag GmbH Berlin Heidelberg and Guangdong Science and Technology Press, Guangzhou, p 276

Xie ZD, Sharp TG (2007) Host rock solid-state transformation in a shock-induced melt vein of Tenham L6 chondrite. Earth Planet Sci Lett 254:433–445

Xie XD, Chen M, Wang DQ (2001a) Shock-related mineralogical features and P–T history of the Suizhou L6 chondrite. Eur J Mineral 13:1177–1190

Xie XD, Chen M, Wang DQ, El Goresy A (2001b) $NaAlSi_3O_8$-hollandite and other high-pressure minerals in the shock melt veins of the Suizhou L6 chondrite. Chin Sci Bull 46:1121–1126

Xie XD, Minitti ME, Chen M, Wang DQ, Mao HK, Shu JF, Fei YW (2002) Natural high-pressure polymorph of merrillite in the shock vein of the Suizhou meteorite. Geochim Cosmochim Acta 66:2439–3244

Xie XD, Minitti ME, Chen M, Wang DQ, Mao HK, Shu JF, Fei YW (2003) Tuite, γ-$Ca_3(PO_4)_2$, a new phosphate mineral from the Suizhou L6 chondrite. Eur J Mineral 15:1001–1005

Xie XD, Sun ZY, Chen M (2011) The distinct morphological and petrological features of shock melt veins in the Suizhou L6 chondrite. Meteorit Planet Sci 46:459–469

Xie XD, Gu XP, Yang HX, Chen M (2019) Wangdaodeite, the $LiNbO_3$-structured high-pressure polymorph of ilmenite, a new mineral from the Suizhou L6 chondrite. Meteorit Planet Sci 55:184–192

Xie XD, Gu XP, Chen M (2022) The discovery of TiO_2-II, the α-PbO_2- structured high-pressure polymorph of rutile in the Suizhou L6 chondrite. Acta Geochim. https://doi.org/10.1007/s11631-022-00585-4